High-resolution drone lidar for Mediterranean archaeology: point classification, feature detection, and the potential for cultural heritage management

Evan I. Levine
University of Copenhagen
evl@teol.ku.dk

Hallvard Indgjerd
Museum of Cultural History, University of Oslo
hallvard.indgjerd@khm.uio.no

Magne Samdal
Museum of Cultural History, University of Oslo
magne.samdal@khm.uio.no

Steinar Kristensen
Museum of Cultural History, University of Oslo
steinar.kristensen@khm.uio.no

Introduction

The introduction of airborne laser scanning (ALS) or lidar into the archaeologist's ever-expanding toolkit has profoundly impacted our understanding of premodern landscapes. Most notably used for the detection of archaeological sites in densely vegetated environments, airborne lidar has been an effective tool for recording the surface topography of a landscape beneath the upper canopies of forests or jungles.[1] While the collection of aerial lidar data for archaeology has traditionally required significant funding and collaboration with specialist firms, recent developments in lightweight and affordable sensors mounted on unmanned aerial vehicles (UAVs) or drones have increased access to lidar data collection. With drone lidar, archaeologists can now capture smaller areas of interest at much higher resolutions than traditional airborne lidar, enabling precise and efficient documentation of landscapes with complex topography or ephemeral archaeological features. With readily available lidar sensors and medium-payload consumer drones, archaeologists are now able to bring lidar data from new regions into dialogue with more established zones of lidar-based research. Additionally, the higher resolution afforded by low-altitude flights and direct control over data collection enables archaeologists to explore innovative applications of aerial lidar and pose new questions about premodern landscapes.

While well-defined workflows exist for collecting, processing, and analyzing lidar data captured by airplane,[2] the growing use of drone lidar lacks equivalent critical evaluation. To date, there is no established best practice for using drone lidar in Mediterranean contexts, where data quality can vary greatly due to differences in resolution and ground cover. The need for a critical review of drone lidar methods in this context is particularly relevant because – unlike professionally processed lidar data collected by airplane – the proliferation of drone based lidar packages has led

[1] Vinci *et al.* 2024.
[2] Comprehensive guidelines for best general practices for airborne lidar for archaeological data collection and analysis have recently been published by the European Archaeological Consilium (Bennett and Cowley 2025).

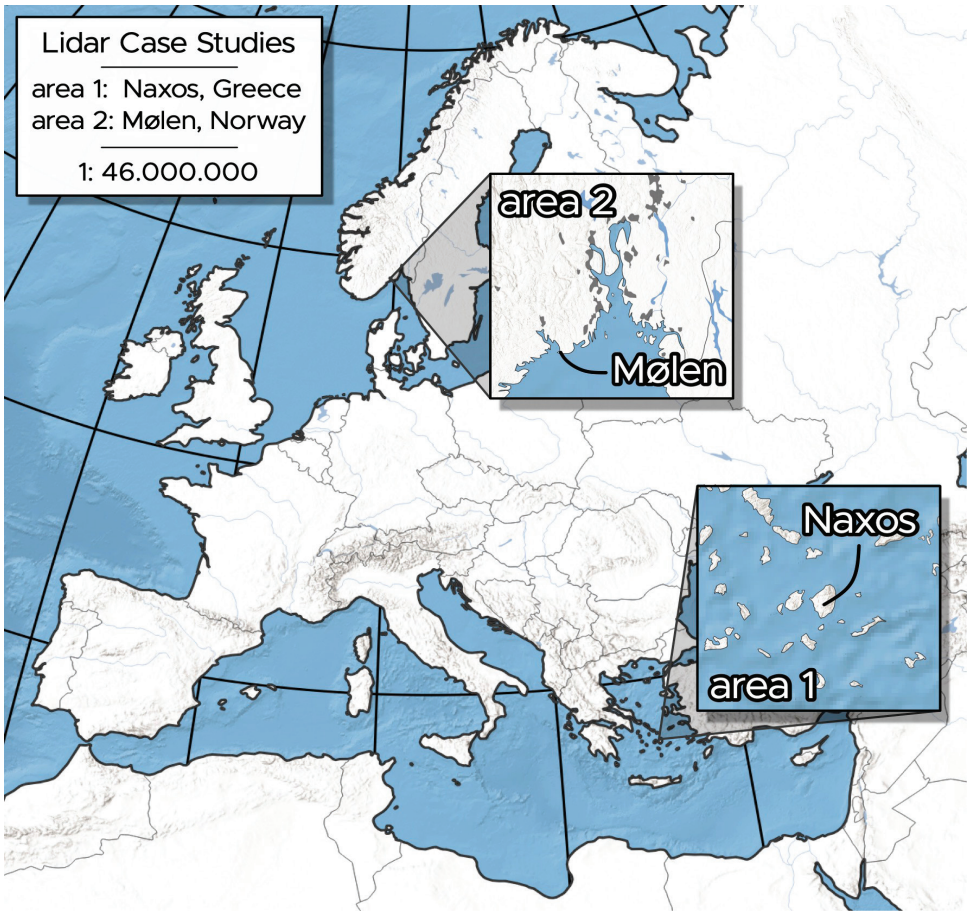

Figure 1. Study areas for this paper including 1) Naxos, Greece and 2) Mølen, Norway

to an increased rate of data collection, processing, and analysis by archaeologists who are not lidar specialists.

This paper critically reviews a range of methodologies for drone lidar data collection and processing in Mediterranean archaeology, providing a systematic evaluation of their effectiveness for recording surface topography.[3] To contextualize these findings, the results are compared to those of drone photogrammetry, a more ubiquitous, established, and cost-effective method. The primary case study examines data collected by the Naxos Quarry Project, an interdisciplinary survey of ancient marble quarries on the Cycladic island of Naxos in an area characterized by diverse vegetation, complex topography, and varied anthropogenic features (Figure 1, area 1). These findings are contrasted with data from the coastal Iron Age funerary landscape of Mølen in southern Norway, a non-Mediterranean environment with comparable vegetation profiles and similarly complex archaeological features (Figure 1, area 2). A multi-year campaign of lidar data collection at Mølen highlights the effectiveness of these data for mapping physical change over the long term at high resolution. Comparing data between Naxos and Norway offers key insight into the particularities of drone lidar data for archaeological documentation and the need to

[3] While this study focuses solely on the viability of available data collection strategies, classification algorithms, and software packages for low-altitude remote sensing of sparsely vegetated archaeological landscapes, we note the need for a similar review of the visualization and analysis of the resultant rasterized digital elevation models remains beyond the scope of the paper. Existing initiatives for archaeological raster analysis, like the open-source Relief Visualization Toolbox (RVT), offer useful and well-tested tools for lidar-based elevation models. As is the case for classification models, however, these tools are specifically designed for coarser airborne datasets. We encourage future efforts to focus on how such visualization tools can be optimized for the additional requirements of high-resolution elevation models.

adopt workflows that are appropriate for both the region where one works and the mode of data collection in use.

Background: aerial data in archaeology and the development of drone lidar

Traditional uses of aerial photography and remote sensing in archaeological fieldwork include feature identification and site documentation using orthorectified photographs from airplane, balloon, or satellite, while multispectral or thermal imagery has been used to document environmental factors or subsurface architectural features.[4] Advances in aerial lidar for archaeological documentation in highly vegetated environments like jungles and boreal forests have illuminated expansive remains in previously undocumented or understudied parts of the Americas,[5] Europe,[6] and Southeast Asia.[7] Widespread news coverage and public interest in these studies has served to popularize aerial lidar, leading to increased funding for projects that integrate lidar prospection into their broader fieldwork strategies.[8] This has encouraged archaeologists to develop use cases for lidar in diverse landscape types, ecosystems, and for a wider range of applications than its well-known ability to penetrate vegetation.[9]

While earlier archaeological projects required significant funding to commission aerial lidar data collection, increasing access to countrywide open source lidar datasets in North America and Europe has prompted the development of several large-scale systematic studies with a range of research questions that have reshaped our understanding of human activities in these regions.[10] Meanwhile, the lack of comparable datasets for archaeologists working in African, South American, Asian, or Eastern Mediterranean contexts has resulted in an uneven application of lidar in these regions, with particular implications for local cultural heritage management and archaeological services and broader implications on the development of comparative, multiregional datasets.[11]

Archaeologists have most commonly engaged with lidar datasets collected by airplane at relatively high altitudes, maximizing the spatial coverage of a particular collection for a given budget and pushing lidar-focused archaeological study toward macro-regional or regional study areas.[12] While data collection strategies vary, the average resultant resolution of elevation data with which archaeologists actually engage is close to 1m,[13] representing a substantial increase in data quality from the radar-derived orbital elevation or visual datasets most often employed for archaeological study.[14] At this resolution, archaeologists have used lidar to accurately map complex networks of agricultural terracing, road networks, urban architecture, water management systems, and

[4] Bewley 2003.
[5] Canuto *et al.* 2018; Prümers *et al.* 2022.
[6] Norstedt *et al.* 2020; Bernardini and Vinci 2020.
[7] Evans *et al.* 2013; Evans 2016; Chevance *et al.* 2019.
[8] See Handwerk 2022 reporting on Prümers *et al.* 2022, Rannard 2024, reporting on Auld-Thomas *et al.* 2024, and Georgiou 2024, reporting on Frachetti *et al.* 2024.
[9] Recent studies have demonstrated the efficacy of airborne lidar for site detection in sparsely vegetated upland or mountainous areas of Italy (Fontana 2022) and Uzbekistan (Frachetti *et al.* 2024), the development of green lidar for bathymetric mapping offers the opportunity to detect underwater archaeological sites (Hale *et al.* 2023.), and an increasing number of projects are training machine learning algorithms with lidar data for the predictive modeling of archaeological landscapes (Verschoof-van der Vaart *et al.* 2020; Cody and Anderson 2021; Guyot *et al.* 2021; Carleton *et al.* 2023).
[10] See Vinci *et al.* 2024 for a review of open access countrywide lidar datasets and the implications for these data on archaeological research.
[11] Uneven access to funding, equipment, and open access datasets has led to imbalances in the global adoption of these tools and the development of a so-called 'lidar elite' in some regions (Cohen *et al.* 2020: 78).
[12] In mediterranean contexts, Fontana 2025 offers a thorough review of the effectiveness of lidar analysis on a macro-regional (15,296 km^2) study area using 1m^2 resolution elevation data, while Sporn and Kennedy in this volume (735 km^2 at 0.25 m^2 resolution), Fachard *et al.* in this volume (200 km^2 at 0.25 m^2 resolution), and Matsas, *et al.* in this volume (80 km^2 at 0.25 m^2 resolution) each present case studies for the application of high altitude aerial lidar for smaller regional study areas as commonly deployed in Greek archaeological contexts.
[13] The 291 archaeological projects reviewed by Vinci *et al.* 2024 presented an average study area of 1518 km^2, an average lidar ppm sampling strategy of 33.1, leading to an average topographic data resolution of 1.1m. While this study is not entirely comprehensive, it is representative of the most common resolution ranges of aerially collected lidar datasets used in archaeological research.
[14] At present, 3m elevation data collected by the Italian Space Agency's COSMO-SkyMed Synthetic Aperture Radar (SAR) represents the highest resolution widely accessible orbital elevation dataset that has been utilized for archaeological research (Tapete *et al.* 2021).

other anthropic features at a speed and scale that was previously unimaginable. Lidar analysis at this scale is most effective at recognizing and documenting relatively large, regular features with linear or ovoid characteristics like terraces or large enclosures.[15] The co-development of a rigorous ground truthing research plan is a critical component in the accurate identification and interpretation of identified features and patterns.[16]

While most archaeological lidar projects make use of more established aerial platforms for data collection, several recent studies have highlighted the utility and benefits of drone lidar for site documentation and prospection. This accompanies the almost ubiquitous adoption of drones for a wide range of archaeological documentation techniques. Following pioneering work on drone photogrammetry by Eisenbeiss and colleagues, drone imagery has enriched, facilitated, and democratized aerial documentation by archaeologists.[17] This phenomenon was prompted by rapid developments in multi-rotor consumer drone technology and increasingly intuitive user interfaces and flight planning software packages throughout the 2010s.[18] These developments encouraged a fundamental shift in the use of these tools from specialist or hobbyist communities to widespread use – offering archaeologists a low-cost, quick, and relatively straightforward option to collect project-specific, high quality aerial data.[19] Two parallel developments were instrumental in the widespread adoption of drones for archaeological data collection: (1) increasing access to low cost GNSS hardware like DGPS units allowed these data to be accurately georeferenced across entire landscapes;[20] and (2) parallel developments in 3D modeling software based on the principles of photogrammetry meant that the photographs collected by consumer drones could be quickly and easily processed to record landscapes, structures, and excavations in three dimensions with an unprecedented level of data quality.[21] Together, these tools offer archaeologists the ability to generate rasterized data like orthorectified photomosaics and digital elevation models that could be integrated into fieldwork-related GIS projects.

The earliest adoption of drone lidar for archaeology took place in densely vegetated jungle or forest environments in Mesoamerican, Amazonian, and northern European contexts, where aerial lidar has been shown to be most effective.[22] While these early studies highlighted the research and documentation potential of the increased resolution of lower altitude drone lidar, the costs of these platforms and limitations in processing power and battery capacity limited their potential for widespread adoption. The adoption of these tools for archaeological prospection and documentation in Mediterranean environments is a more recent phenomenon, with experimental studies testing the efficacy of drone lidar to penetrate the low, thick vegetation encountered in Italian contexts and the implications for these methods elsewhere in the region.[23] In each case, these studies are presented as preliminary and exploratory, focused on the documentation of relatively large-scale architecture at known sites beneath high vegetation. In so doing, they deploy drone lidar platforms for a similar purpose as aerial lidar at a smaller scale with an increased resolution. By contrast, the papers collected in this volume highlight the variance in data collected by aerial and drone lidar, making use of the increased resolution, greater control over data collection and processing, and limitations in areal coverage to ask new questions that are more appropriate for data of this scale, resolution, and type.[24]

[15] Knodell *et al.*, in this volume.
[16] Garrison *et al.* 2023; Manquen *et al.* in this volume.
[17] Eisenbeiss *et al.* 2005; Eisenbeiss and Zhang 2006.
[18] The release of the Phantom quadcopter by DJI in 2013 marked a fundamental shift in access to high quality and reliable UAV platforms with simple and intuitive user interfaces.
[19] Hill 2019.
[20] Hill *et al.* 2019.
[21] Sapirstein and Murray 2017.
[22] Khan *et al.* 2013; Risbøl and Gustavsen 2018; Murtha *et al.* 2019; McCoy *et al.* 2021.
[23] Balsi *et al.* 2021; Calderone *et al.* 2024.
[24] See Garcia Sanchez *et al.* in this volume on Valley of the Muses; Pike *et al.* in this volume on Mt Pentele; Waagen *et al.* this volume on Halos.

Methods and equipment

Technical specifications and data collection

Data for both case studies were collected using two DJI quadcopter platforms: the Matrice 300 and the Mavic 3 Enterprise. The Matrice 300 was equipped with the Zenmuse L1 lidar module, which incorporates a 20-megapixel optical sensor for concurrent RGB photography (Figure 2). This combination provides a compact, flexible, and relatively low-cost solution for lidar data capture. However, its takeoff weight of 7.2 kg and wingspan of just over a meter require additional operator licensing, and it is less mobile compared to the 951g Mavic 3, which is equipped with a 20-megapixel wide-angle lens for RGB photography.

The L1's Livox Mid-70 lidar sensor can record up to three target echoes (returns) at a collection rate of 480 KHz, with two or three returns per point.[25] Automated flight paths can be calculated and executed from the DJI flight controller software, in addition to sensor calibration patterns based on the pilot's requested parameters for area coverage, resolution, overlap, and flight speed. SRTM elevation data with 30m resolution was downloaded to make use of consistent above ground level (AGL) altitude data collection. However, flights at low altitude and in areas with steep topographic change meant that SRTM data were in some cases too coarse to provide reliable AGL flight plans, and consistent altitude flights were subsequently employed.

Figure 2. Equipment used for this study (clockwise from top left): DJI Matrice 300 RTK, DJI Mavic 3E RTK, Emlid Reach RS3 GNSS RTK as a rover for field survey, Emlid Reach RS2 GNSS RTK as a base

[25] DJI, 2023: 5.

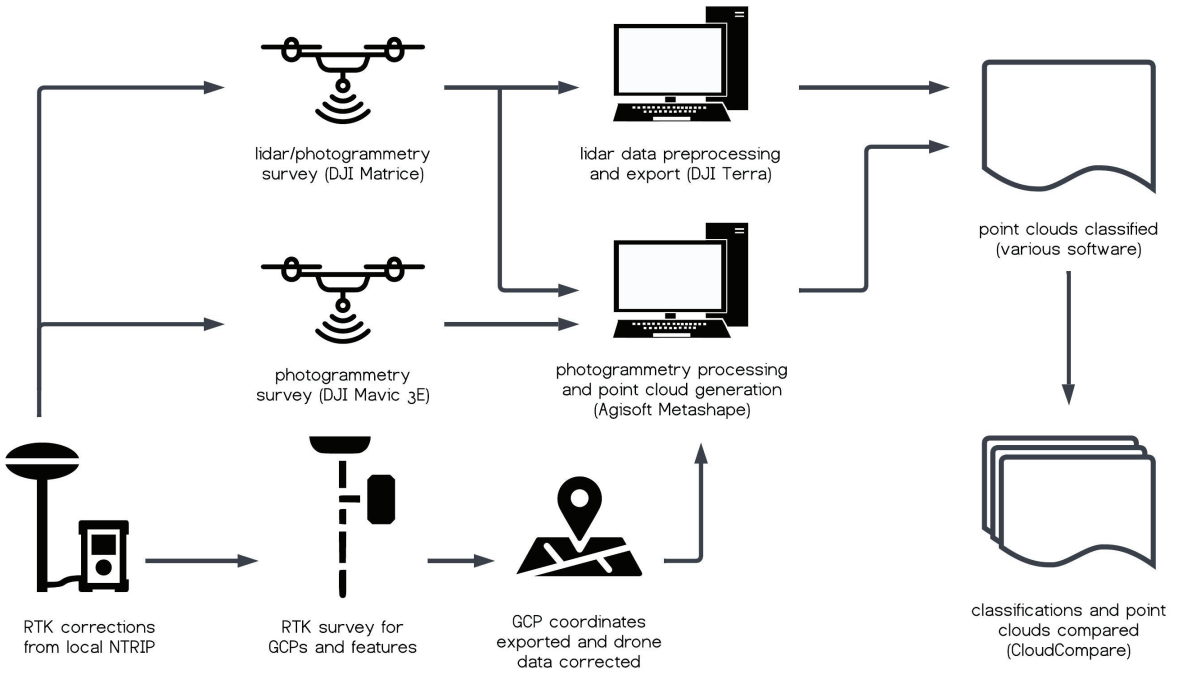

Figure 3. UAV data collection and point cloud processing workflow

Both UAVs were equipped with Real-Time Kinematic (RTK) GNSS positioning systems, which enabled accurate recording of the sensor's position within 2–3cm without the need for Ground Control Points (GCPs) or any post-processing.[26] On Naxos, RTK corrections were provided by an ad-hoc base station set up with an Emlid Reach RS2 GNSS receiver broadcasting NTRIP data via Emlid's NTRIP Caster software. An Emlid Reach RS3 receiver, receiving the same corrections, was used for terrestrial measurements of coded photogrammetry targets, which served as GCPs to assess RTK reliability and provide additional accuracy control. At Mølen, correction data was provided by the Norwegian Mapping Authority's CPOS positioning service which calculates a virtual reference station based on permanent geodetic stations.[27]

Data processing workflow

Like most commercial lidar sensors, the L1 collects data in a proprietary format that requires the use of DJI Terra software for initial processing and export into common point data formats.[28] In the first step of the study, data for each flight were exported with minimal changes as LAS point clouds, providing a baseline dataset for evaluation of different processing methods (Figure 3). Photogrammetry data went through pre-processing in Agisoft Metashape, which consisted of image alignment, reference point input, alignment optimization and point cloud generation, all at the 'high' quality setting. The resulting point clouds were then exported as LAS files. Comparative lidar datasets from Mølen were downloaded from the public Norwegian lidar and elevation data repository, Høydedata,[29] and from the Norwegian Institute for Cultural Heritage Research (NIKU).

Point clouds consist of unorganized, dimensionless points with a position in 3D space given as Cartesian X, Y, and Z coordinates. Additionally, each point may include one or more properties containing further information, or metadata, such as RGB color values, normal vectors, time of capture, return number, or material class. Lidar capture produces point clouds by default, with metadata

[26] Ekaso *et al*. 2020.
[27] Kartverket 2017
[28] See also Waagen *et al*. this volume; Pike *et al.* this volume.
[29] https://hoydedata.no/, operated by Statens Kartverk.

designated during pre-processing depending on sensor capabilities and software preferences. In photogrammetric workflows, dense point clouds are usually an intermediary step in the processing, calculated based on triangulated camera positions and depth maps, and in turn forming the basis for raster Digital Surface Models (DSMs), orthomosaics, and 3D meshes. Recent photogrammetry software may skip dense point cloud generation altogether, unless there is a specific use case for point cloud visualization or analysis.[30] This means that the feature and scalar fields available for point clouds generated by lidar and by photogrammetry differ. Notably, lidar points have no color data, unless colorized based on image capture, and photogrammetric points cannot have return data.

While RGB data are useful for visual inspection, assigning points to distinct classes based on terrain and feature type has clear advantages for filtering and segmentation, bulk analysis, or even machine learning. A standard set of classification values is defined in the LAS format specification,[31] ensuring interoperability across software packages. A typical use case is the classification of points into ground, man-made features and vegetation classes. From this, users can filter out points determined to be vegetation to create Digital Feature Models (DFMs), or the retrieval of only ground points for Digital Terrain Models (DTMs). While the classification can be carried out manually by selecting points and assigning the selection a specific class value, this is labor intensive and not feasible with large datasets. However, automatic classification algorithms have been developed that try to make real-world distinctions based on point positions and recorded metadata, such as the elevation difference to nearby points, return number or color value.[32]

Štular and colleagues developed a methodology optimized for retaining archaeological features in the classification of ALS data and scholars have compared the viability of classification and filtering algorithms for ALS, typically with a resolution of fewer than 10 points/m^2.[33] Creating more nuanced distinctions into specific, archaeologically relevant feature classes for high resolution point clouds remains a challenge. In this study, we focus on creating Digital Feature Models (DFMs) to retain man-made features for archaeological analysis.

Case study 1: Naxos Quarry Project

Naxos area 1 (Melanes)

For our first drone lidar test case, we selected an area under study by the Naxos Quarry Project in a shallow valley between the villages of Melanes and Ano Potamia that offered the typical profile for a Cycladic agricultural landscape, interspersed with traces of ancient marble quarrying.[34] The area is characterized by diverse vegetation and terrain, offering an ideal setting for testing lidar technology (Figure 4). The study aimed to capture a range of terrain features, including open grass fields, dense low maquis, higher open vegetation,

Figure 4. Representative landscape photo of Naxos area 1

[30] See for instance Shuetz 2016 for Potree, a point cloud web viewer commonly used in archaeology and cultural heritage management.
[31] ASPRS 2019: 29-30.
[32] See Štular and Lozić 2020: 6-7 for a concise overview of the mathematics behind different point cloud classification algorithms.
[33] Štular *et al.* 2021: 17-18; Podobnikar and Vrečko 2012; Julge *et al.* 2014.
[34] Levitan *et al.* forthcoming.

freestanding trees, terracing, stone walls, and buildings. Two areas were delineated for repeat, structured flights. The smaller area (measuring 70 x 100m, Figure 5, area 1) was resampled eight times in total with variations in recorded returns and flight altitude (Figure 6).

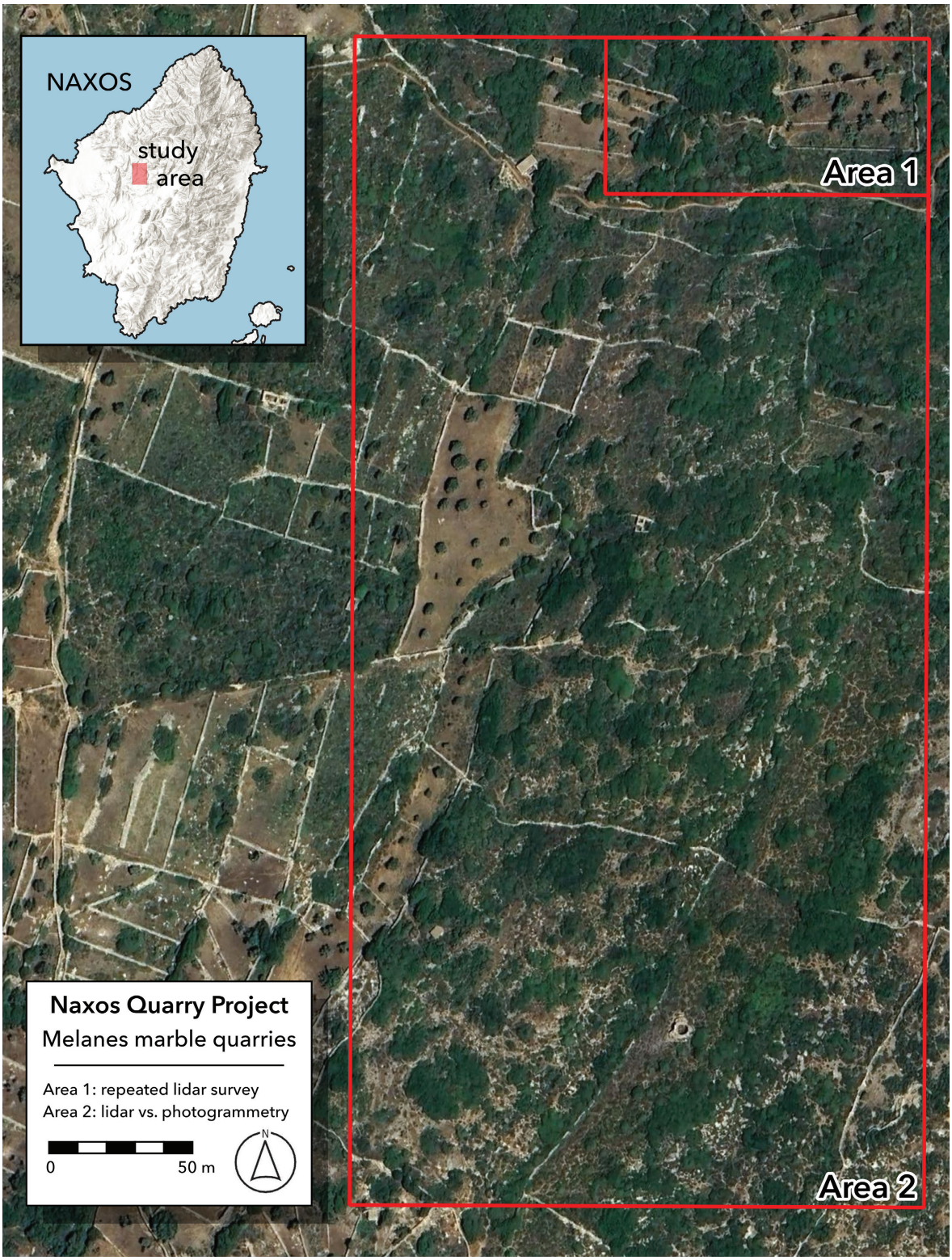

Figure 5. Areas of the Melanes Marble Quarries selected for repeated lidar survey under different parameters (Area 1) and for comparison between lidar and photogrammetry (Area 2).

Height	Returns	Total Points	1st return	2nd return	3rd return	avg res (pts/m2)	Area (m2)	Khz
30	2	38,871,945	96.22 %	3.78 %		5571	6978	240
30	3	24,347,497	96.05 %	3.84 %	0.11 %	3489	6978	160
50	1	12,907,442	100%			1850	6978	240
50	3	9,243,824	96.03 %	3.84 %	0.13 %	1325	6978	160
60	2	14,840,737	96.69 %	3.31 %		2127	6978	240
60	3	9,783,074	96.17 %	3.70 %	0.13 %	1402	6978	160
90	2	5,271,982	97.44 %	2.56 %		756	6978	240
90	3	3,581,754	97.53 %	2.43 %	0.04 %	513	6978	160

Figure 6. Table of flight parameters for UAV documentation of Naxos area 1

As shown in figure 6, the proportion of second returns increased when the flight altitude was lowered from 90 to 60 meters AGL, yet the difference between 60 and 30 meters was much less distinct. In all cases, multiple returns were predominantly recorded in areas with free-standing olive trees or other medium-high vegetation, while very few additional return signals were recorded in the low maquis growth. The density of second returns is similar in the data from the three-return flights and third returns were sparse. This suggests that the sacrifice in overall resolution in three-return flights for the possibility of reading an extra return, may not provide significant advantages in these landscape types.

Despite limited vegetation penetration overall, pre-trained classification algorithms allowed us to separate the data into meaningful classes for further analysis. We tested nine available and commonly used classification algorithms on point cloud data from the 30-meter, three-return flight to evaluate their effectiveness for Mediterranean lidar data processing (Figure 7). The algorithms yielded varied results: some only classified ground points, while others separated the data into multiple classes for natural and man-made features. To isolate ground points, we excluded points classified as vegetation (low or high) before generating Digital Feature Models (DFMs). A Digital Surface Model (DSM) that included all points, without classification or return filtering, was generated in Metashape as a baseline comparison (Figure 7, A). The DSM shows the dense vegetation cover at different heights, with low maquis in the south, higher bushes and small trees in the north-west, and freestanding olive trees in the northeast and southwest. The footpath and unobscured stone walls are clearly visible.

Metashape's built-in classifier uses six predefined classes, from which we could generate a DFM that successfully removes the free-standing olives but preserves very little information in the areas with low and medium maquis cover (Figure 7, B). By comparison, executing the same process for data from the 60m, 3-return flight produces a similar result to the 30m dataset (Figure 7, C). However, considerably less ground data is preserved in areas with medium vegetation cover when compared to the 30m dataset, contradicting our assumptions based on visual inspection of return data.

DJI Terra, the software used to read and export the L1 sensor's raw data, includes a pre-trained classification function with nine classes.[35] The DFM generated from this classification resulted in some smudging and artificial edges but recovered a good cover of ground points (Figure 7, D). Some

[35] These are 1) ground, 2) low vegetation, 3) medium vegetation, 4) high vegetation, 5) building, 6) poles), 7) wire, 8) water, and 9) unclassified.

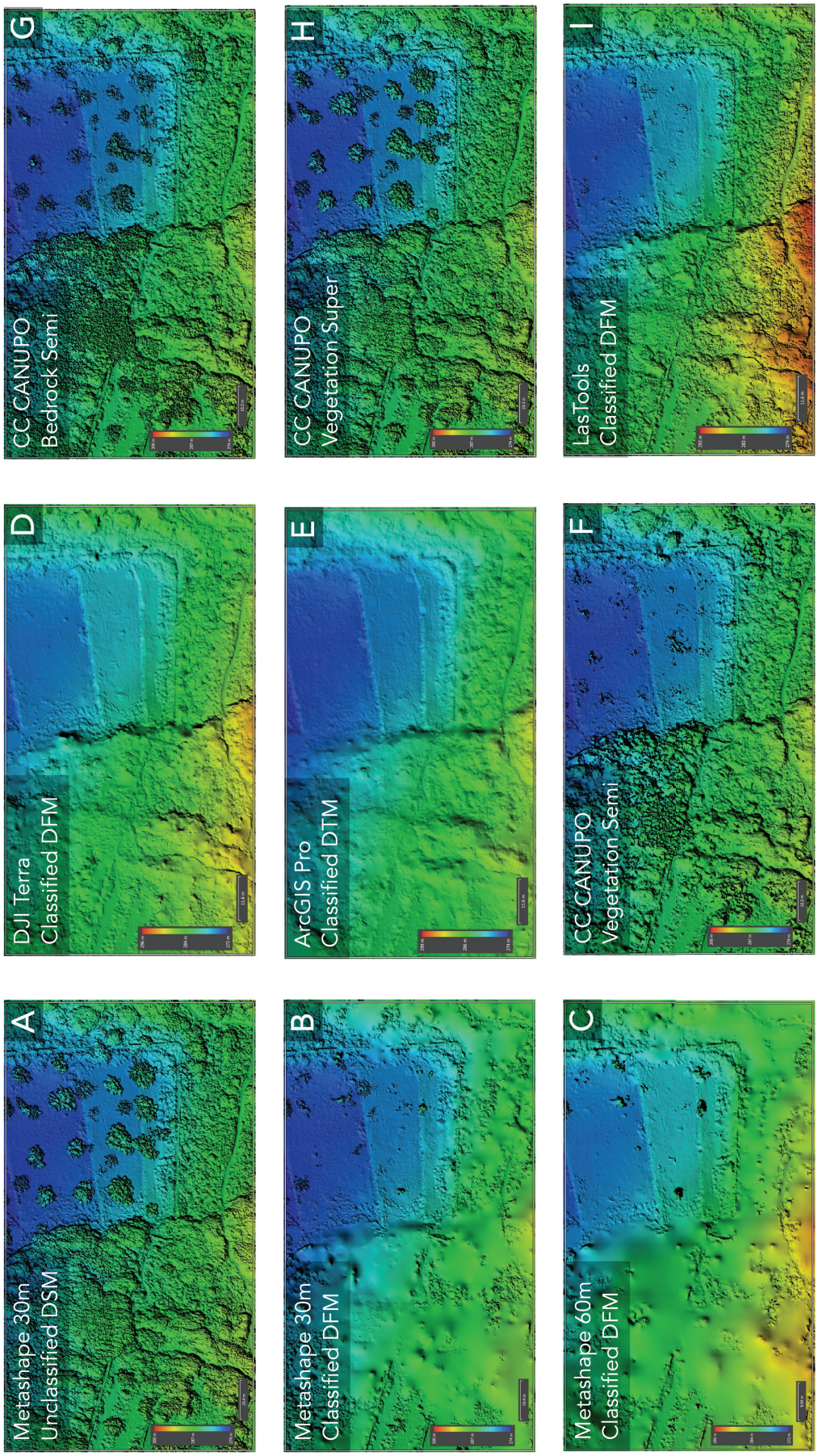

Figure 7. Results of the tested classification models for lidar point clouds collected at Naxos area 1

features, like the stone wall in the southwest, running below the vegetation, are discernible even if only as negative impressions.

The built-in ground classification tool in ArcGIS Pro is a binary classifier dividing the point cloud into ground and unclassified points. It is effective at creating a traditional Digital Terrain Model by removing all points classified as non-ground. However, this result also excludes many features of archaeological interest, this means that the features we are interested in also disappear (Figure 7, E). Nevertheless, this tool serves as a good starting point for further classification and refinement.

While the aforementioned commercial classification algorithms offer limited options for adjustments and user refinement, the CANUPO (CAractérisation de NUages de POints) project has developed an open-source toolbox based on characterization of geometric properties for the classification of point clouds.[36] It has the advantage of being built for Terrestrial Laser Scanning (TLS) data, which are captured at distances and resolutions much closer to drone lidar. As it only considers geometry, and not color, return number, or other scalar data fields, a CANUPO based classification should handle photogrammetry and lidar point clouds in exactly the same way. While an aging package, the user-friendly interface for supervised training of custom classifiers makes CANUPO a useful tool in developing and testing new recording methods. We tested three different pre-trained classification models – Vegetation Semi (Figure 7, F), Bedrock Semi (Figure 7, G), and Vegetation Super (Figure 7, H) – using the CANUPO plugin for Cloud Compare. These were all more conservative than the other models used, trained to target a specific subset of topography, and would be better employed in combination. However, the Vegetation Semi classification was particularly effective at removing the medium high maquis.

LasTools is a collection of open and closed source point cloud processing tools and algorithms developed by rapidlasso.[37] We used a combination of *lasground*, *lasheight*, and *lasclassify*, which were run through the LasTools QGIS plugin. Lasground is a binary classifier dividing the points into ground and non-ground points. It has options for specifying terrain and scale-based parameters, like steepness and feature height, to fine tune the algorithm to the input data. The lasheight tool computes the height above ground of non-ground points and stores the data in a scalar field for use in the next step. Finally, lasclassify combines elevation and neighbor geometry information to classify vegetation and features based on height and ruggedness. While a relatively rudimentary approach, the ability to adjust parameters and check intermediate results at multiple stages in the process gives the user greater control over the outcome. Of our tests, the LasTools pipeline produced the best combination of vegetation penetration and preservation of non-vegetation features, creating a sharp DEM with little interpolation and smudging (Figure 7, I).

Naxos area 2 (Melanes)

To compare the results of drone lidar and drone photogrammetry in a Mediterranean environment, we designated a larger, 50 ha area for three flights at 100 m AGL (Figure 5, area 2). This area encompassed Area 1, extending southward to include additional features like footpaths and outfield vegetation zones (Figure 8). Two flights captured lidar data with 50% overlap with one and three returns. A third flight captured the same area only with RGB photography taken with the L1 sensor's integrated camera for photogrammetry. These were then processed into a high-quality point cloud using Agisoft Metashape based on depth maps. Point clouds for all three flights were classified using Metashape's built-in classifier, and DFMs were generated by excluding high vegetation.

[36] Brodu and Lagur 2012.
[37] https://rapidlasso.de

A side-by-side comparison of the DFMs from lidar and photogrammetry showed minor differences, mainly in areas of freestanding, higher vegetation (Figure 9, A-D). In more than 96% of the surveyed area, the difference between surface models based on lidar and photogrammetry are within ±2 cm (Figure 9, E). To assess the ability of the method to penetrate vegetation, difference-rasters were calculated by subtracting each flight's DSM from its corresponding DFM (Figure 9, F-H). Positive values (orange-red) indicate areas of vegetation removal, while green areas show no change.

Both lidar and photogrammetry struggled to reconstruct the ground under dense, low maquis, but photogrammetry performed well around the edges of the vegetation patches areas due to the oblique photo capture angle. Considerably better results are noted in the lidar data in the open areas with free-standing trees in the northern parts of the view. This indicates that a lower-altitude photogrammetry flight with a stronger oblique angle would improve the ability to recover ground under such vegetation. A calculation of

Figure 8. Representative landscape photo of Naxos area 2

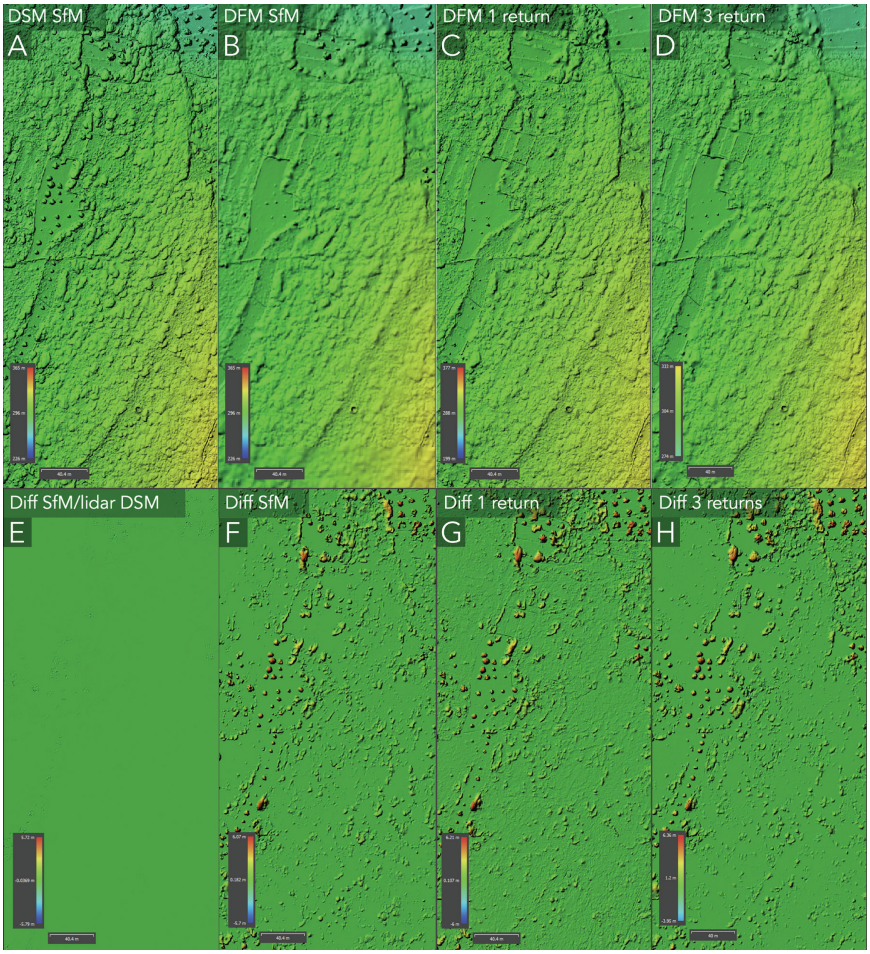

Figure 9. Comparison of photogrammetry and lidar DSM/DFMs (top) and difference calculations between photogrammetry and lidar datasets (bottom)

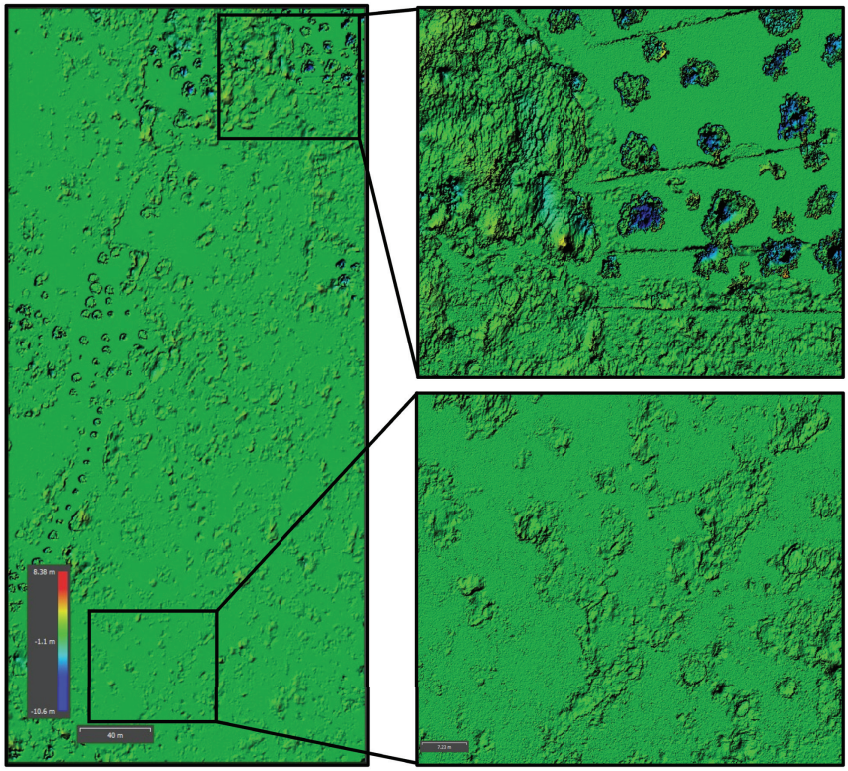

Figure 10. Areas of different (blue) and equivalent (green) elevation between a section of the single return lidar DSM/DFM difference map and the photogrammetry DSM/DFM difference map

the difference between the results from the single return lidar DSM/DFM difference map and the photogrammetry DSM/DFM difference map (Figure 10) further illustrates the comparison. In the northern area, the two methods have more than 15 cm recorded elevation difference in 42% of the area, against only 11% in the southern area. This highlights that lidar is most effective compared to photogrammetry in areas of higher and more open vegetation, while differences are minimal in areas with dense, low vegetation.

Analysis of the classified and processed lidar and photogrammetry elevation data collected at Melanes revealed a series of previously undocumented archaeological features throughout the study area. In addition to areas of premodern terracing and architecture, high resolution drone lidar data proved particularly effective at generating surface elevation data in areas of high vegetation that was instrumental in the identification of areas of ancient marble extraction and the topographic signatures of ramps and slipways that were constructed for the movement of extracted blocks. Each area identified through lidar analysis was flagged for in person ground truthing and documentation. Meanwhile, lidar and photogrammetry generated similar elevation datasets in areas of dense lower vegetation, although both proved useful in guiding subsequent fieldwork and documentation in these areas. These results highlight the benefits of collecting and processing high resolution drone lidar for particular environmental conditions in micro-scale Mediterranean landscape archaeological projects, while reinforcing the effectiveness of low altitude drone photogrammetry with oblique image capture for a wider range of landscape vegetation profiles at this scale.

Case study 2: Iron Age graves **(Mølen, Norway)**

While our first case study focuses on the vegetation penetration potential of drone lidar in Mediterranean landscapes, our second case study highlights how the classification and analysis of drone lidar data can be placed in dialogue with other ALS and photogrammetric datasets for cultural heritage management and protection. Focusing on the Mølen Archaeological Park in coastal southern Norway, we highlight how lidar can aid in the detection of both human interventions and

Figure 11. The archaeological and coastal landscape of the Mølen Iron Age tombs

natural processes in environments with similar geological and vegetation profiles to Mediterranean contexts.

Mølen is the southwestern tip of Raet, the longest Scandinavian terminal moraine formed towards the end of the last glacial period. The area is covered in a thick layer of cobbles and small boulders, the remains of moraine masses where smaller particles have been washed out by the sea. The archaeological site consists of 230 mounds and cairns ranging from 1 to 35 meters in diameter believed to date from the 1st millennium CE (Figure 11).[38] Though legally protected, it remains a popular recreational area, resulting in landscape wear and the construction of cairns and windbreaks from the local stone.

The site has been documented by aerial photography repeatedly since 1959,[39] and has more recently been covered by several ALS campaigns. The current analysis uses the four ALS datasets with a resolution of 5 points/m^2 or higher recorded between 2008 and 2022 as comparison data for our UAV lidar scan (Figure 12). Nesbakken and Risbøl[40] conducted a similar Change Detection Analysis using the 2008 and 2010 DEMs, combined with a manual analysis of seven aerial photography datasets. They were able to identify changes in elevation of more than 10 cm in seven of the main mounds, six of which showed a central build up and material disappearing from the side or base, compatible with a known restoration and reconstruction project in 2009.[41]

For this study, DSM rasters were generated from each dataset's point cloud and used to calculate difference rasters between the 2024 data and each earlier lidar recording. These rasters were

[38] Berge 2009: 17-18.
[39] 11 orthomosaic datasets available at www.norgeibilder.no, a public portal for rectified geodata.
[40] Nesbakken and Risbøl 2014.
[41] Nesbakken and Risbøl 2014: 140-142; Berge 2009.

Year	Resolution (pts/m2)	Method	Sensor	Publication
2008	10	Helicopter, 500m agl	Leica ALS 50-II	Solli 2008
2010	22	Helicopter, 450m agl	TopEye S/N 7	Blom Geomatics 2010
2017	5	ALS	Riegl VQ-1560i	Torsnes 2017
2022	10	ALS	Riegl VQ-1560ii-S	Gustafsson 2022
2024	1109	UAV, 50m agl	DJI L1	

Figure 12. Table showing aerial documentation of the Mølen Iron Age Tombs

visualized in ArcGIS Pro, highlighting the period of material addition and removal (Figure 13, top). A second visualization was made comparing the full spectrum of change between 2008 and 2024, with areas of increasing elevation shown in cyan/blue and material removal in red (stepped at 0.15–1m, Figure 13, bottom). To aid the association of changes with recorded mounds, polygons of recorded monuments were added using the open API of the Directorate of Cultural Heritage, and the orthomosaic from the photogrammetry recording was used as a background layer.

The lower point density of the earlier ALS datasets (5-22 points/m²) caused some interpolation of larger surfaces, leading to smoother elevation models compared to the denser drone lidar data (1000+ points/m²). This difference in point density generated more noise in comparisons between datasets with varying resolution. This required the introduction of a *larger* buffer margin than the one used by Nesbakken and Risbøl, hiding recorded elevation differences of less than 15 cm, versus the 10 cm used in the earlier comparison. Risbøl elsewhere argues for diminishing returns with resolutions above 5 points/m².[42] However, that is within the framework of traditional ALS lidar recording working on averaged surfaces. The low altitude UAV resolution is high enough to track individual stones down to cobble sizes.

Our analysis recorded a total of 169 changes from 2008 to 2024, which included clearly identifiable human-made alterations to existing mounds and the construction of new cairns, pits, and embankments by visitors to the site. The official reconstruction efforts in 2009 noted by Nesbakken and Risbøl were confirmed in our data. The section of the site shown in Figure 13 highlights some typical alterations. Material has been removed at several spots along the top of the long, ship-shaped mound, and redeposited further down its sides (alterations 2-6). Alteration 20, to the east, is the buildup of a windbreak, which was primarily constructed between 2010 and 2017, with some further material removal between 2017 and 2022. Finally, alteration 11 and 12 shows a new cairn being raised using stones from existing, protected cairns after 2022.[43] This is the only major change in the last two years.

The results from Mølen highlight the effectiveness of drone lidar for monitoring long-term changes in archaeological sites, capturing both natural and human-induced alterations with high precision. It also exhibits the effectiveness of comparing elevation datasets collected by different lidar sensors and under a range of data collection parameters. As airborne and drone lidar workflows become increasingly integrated within the toolkits of archaeologists working in Greece and the Mediterranean more broadly, the resultant datasets can be deployed not only to guide feature detection and regional study but will serve as important benchmarks to monitor landscape change and cultural heritage management. For this purpose, the analysis of both large-scale aerial and low-altitude drone lidar datasets can be used to effectively identify areas at risk of natural or

[42] Risbøl and Gustavsen 2016: 20-23.

[43] A yearly monitoring program is planned, using the same equipment and parameters as the 2024 documentation. This will provide point clouds with directly comparable resolutions, which allows for testing of the sensor's precision and accuracy and provide tracking of smaller scale changes.

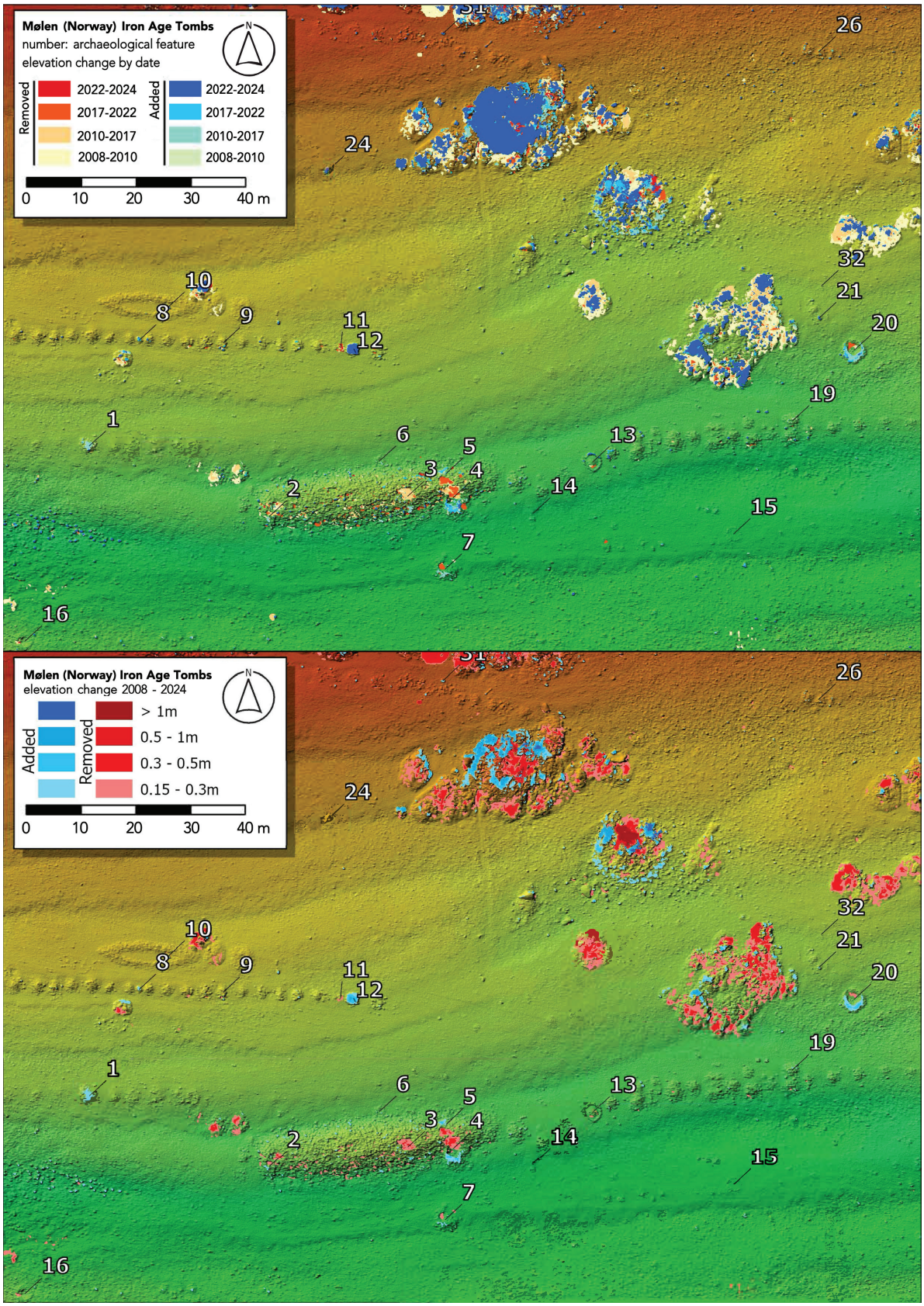

Figure 13. Change detection rasters showing elevation change by date (top) and total positive or negative difference (bottom) at the Mølen Iron Age Tombs

anthropic change. However, we argue that drone lidar platforms will play a key role for tracking landscape change and overall archaeological site preservation, as they offer a cost effective and nimble solution for the repeated data collection of particular study areas required to undertake effective change detection analysis over the long term.

Conclusions

The use of drone lidar in both case studies highlights the utility of this tool for capturing detailed topographic data for archaeological research, particularly in areas where higher altitude aerial lidar may be too coarse for effective data collection. On Naxos, drone lidar was particularly effective at penetrating higher vegetation and identifying linear features like terracing and stone walls, while in Mølen, it provided precise elevation models of archaeological features that can be used to track change over time. However, drone lidar was less effective in areas of dense, low vegetation, where sensor penetration was often limited. In both instances, choosing the most effective classification strategy increased the utility of these data and their potential for archaeological study and documentation.

One challenge encountered in testing industry-standard automated classification models is that many existing algorithms are optimized for high-altitude, low-resolution manned-aircraft lidar data (traditional ALS). While the principles remain the same, the features we aim to capture and how they appear in drone lidar data are different, resulting in misclassification and overlooked features. In some instances, these algorithms still produced useful results, albeit with some misclassifications (e.g., stone walls being identified as cars by Metashape's built-in classifier). These results highlight the importance for archaeologists working with lidar data processing to develop familiarity with a range of classification tools, and how the use of a combination of classifiers on the same dataset may provide the most useful results for their research questions. Moreover, limitations in the classification of drone lidar data with existing models highlights the urgent need for algorithms specifically targeting both close-range aerial lidar, and archaeological features visible at this scale.

Recent advancements, such as the development of 3DMASC (3D Multi-Attributes, Multi-Scale, Multi-Cloud), offer promising new tools for the classification of complex low-altitude datasets.[44] 3DMASC is available as a plugin for CloudCompare, presenting a GUI for supervised training of a classifier, albeit with a considerably higher learning curve than similar platforms. 3DMASC was shown to outperform available classifiers on complex datasets and uses a far broader spectrum of input data than CANUPO,[45] highlighting the potential of this tool for the development of custom low-altitude archaeological classifiers. A different, low-level approach using machine learning for unsupervised or hybrid semi-supervised techniques for training classifiers with neural networks is worth investigating further.[46] Pipelines based on these approaches are likely to be able to produce highly specified classifiers for a variety of data contexts without the need for large pre-labelled training sets.

While drone lidar systems have made the technology more accessible to a broader archaeological audience, the affordability, mobility and ease of use of drone photography for photogrammetry is still unparallelled. To justify the investment in lidar workflows over photogrammetry, the gains in research output need to be substantial. Such benefits have been convincingly presented in wooded landscapes with a high, albeit penetrable canopy.[47] However, our findings suggest that in arid

[44] Letard *et al.* 2024
[45] Letard *et al.* 2024: 195-197.
[46] Several python-based deep learning frameworks, including pyTorch and TensorFlow, contain libraries for working with point cloud and 3D data. Language-model based coding aids are rapidly making these tools accessible for non-experts.
[47] See, for example, the recent results of Abate *et al.* 2025, based on the classification of low altitude drone lidar data classified to maximize feature detection beneath forest canopy at the site of Torre Castiglione in Puglia.

Mediterranean landscapes with dense maquis vegetation or in open coastal landscapes like Mølen, photogrammetry often produced point clouds with accuracy nearly identical to those from lidar, with slightly higher horizontal resolution. This aligns with similar findings in areas like urban parks.[48] In such environments, the ability of lidar to penetrate dense vegetation is not significantly superior to photogrammetry, although with continued advancements in hardware and operator experience, it may still provide advantages in certain contexts. As expected, the photogrammetry data showed little ability to map ground points below the vegetation, but low and strongly oblique image capture produced surprisingly good data at the edges and under overhanging vegetation.

The processing time required to produce the initial, unclassified point cloud is considerably shorter with lidar capture and involves fewer user-defined parameters than photogrammetry. However, photogrammetry is able to produce data at lower costs, with the additional benefit of processing flexibility due to its use of standard image formats and text based spatial data, processed using any of a wide range of accessible software packages. This means a number of different software packages can be used in the processing, including F/OSS and free-to-use alternatives, and the raw data can easily be archived and reprocessed in the future.

A notable reminder from our testing is the enhanced level of detail that can be extracted from photogrammetry using point cloud processing and visualization typically reserved for lidar data. This offers the opportunity to highlight the subtle changes in surface topography – like toolmarks, cuttings, or poorly preserved structures – necessary for the documentation, monitoring, and interpretation of archaeological landscapes.

Aerial data collection strategies for archaeological research continue to develop at a rapid rate, with regular advances in hardware platforms and software packages revolutionizing the way that archaeologists record topography, identify areas of archaeological interest, and monitor known sites of cultural heritage. Recent advances in low altitude, high resolution lidar data collection and processing have already left their mark on these initiatives, with many more developments yet to come. Moreover, software developments linked to lidar data processing have the potential to increase the utility of lower cost and more accessible means of aerial data collection like drone photogrammetry. While the low, dense vegetation and rugged topography of Melanes and Mølen do not present the traditional forested or jungle landscapes for which the results of aerial lidar have been most celebrated, they highlight how lidar survey can be used in interesting new ways to detect, document, and monitor cultural heritage across a range of environmental zones.

Acknowledgments

The authors would like to express their gratitude to our colleagues on The Naxos Quarry Project (co-directed by Rebecca Levitan, Evan Levine, Demetrios Athanasoulis, and Irini Legaki), with particular thanks to Vasiliki Anevlavi and our colleagues from the Ephorate of Antiquities of Cyclades for their support and assistance. The present study was supported by King's College London, the Museum of Cultural History at the University of Oslo, and the Cycladic Foundation's Petros Goneos Memorial Fund. We would also like to thank Alex Knodell, Bonna Wescoat, and the American School of Classical Studies at Athens for the opportunity to share this research among a vibrant group of scholars focused on lidar in Mediterranean contexts.

[48] Kersten *et al.* 2022

References

Abate N., R. Goffredo, D. Dato, A. Minervino Amodio, A. Loperte, A. Frisetti, G. Ciccone, S.E. Zaia, M. Sileo, R. Lasaponara and N. Masini 2025. Adopting an open-source processing strategy for LiDAR drone data analysis in under-canopy archaeological sites: a case study of Torre Castiglione (Apulia). *Remote Sensing* 17(7): 1134.

American Society for Photogrammetry and Remote Sensing 2011. *LAS Specification* (ver. 1.4–R15, July 2019): Bethesda, MD: American Society for Photogrammetry and Remote Sensing.

Auld-Thomas L., M.A. Canuto, A.V. Morlet, F. Estrada-Belli, D. Chatelain, D. Matadamas, M. Pigott and J.C. Fernández Díaz 2024. Running out of empty space: environmental lidar and the crowded ancient landscape of Campeche, Mexico. *Antiquity* 98: 1340-1358.

Balsi, M., S. Esposito, P. Fallavollita, M.G. Melis and M. Milanese 2021. Preliminary archeological site survey by UAV-borne lidar: a case study. *Remote Sensing* 13(3): 332.

Bennett, R. and D. Cowley, D. (eds) 2025. *Guidelines for the use of Airborne Laser Scanning (Lidar) in Archaeology (EAC Guidelines 10).* Brussels: European Archaeological Council.

Berge, S.L. 2009. *Gravrøyser på Mølen. Værvågen, 4088/34, Larvik kommune Vestfold*. Oslo: University of Oslo Museum of Cultural History.

Bernardini, F. and G. Vinci 2020. Archaeological landscape in central northern Istria (Croatia) revealed by airborne LiDAR: from prehistoric sites to Roman centuriation. *Archaeological and Anthropological Sciences* 12(133): 1-18.

Bewley, R.H. 2003. Aerial survey for archaeology. *The Photogrammetric Record* 18: 273–292.

Blom Geomatics 2010. *Project report, 1875 Larvik area*. Sollentuna: Blom Sweden AB.

Brodu, N. and D. Lague 2012. 3D terrestrial lidar data classification of complex natural scenes using a multi-scale dimensionality criterion: Applications in geomorphology. *ISPRS Journal of Photogrammetry and Remote Sensing* 68: 121-134.

Calderone, D., N. Lercari, D. Tanasi, D. Busch, R. Hom and R. Lanteri 2024. Tackling the thorny dilemma of mapping southeastern Sicily's coastal archaeology beneath dense mediterranean vegetation: a drone-based LiDAR Approach. *Archaeological Prospection* 32: 139-158.

Canuto, M.A., F. Estrada-Belli, T.G. Garrison, S.D. Houston, M.J. Acuña, M. Kováč, D. Marken, P. Nondédéo, L. Auld-Thomas, C. Castanet, D. Chatelain, C.R. Chiriboga, T. Drápela, T. Lieskovský, A. Tokovinine, A. Velasquez, J.C. Fernández-Díaz and R. Shrestha 2018. Ancient lowland Maya complexity as revealed by airborne laser scanning of northern Guatemala. *Science* 361(6409): eaau0137.

Carleton, W.C., S. Klassen, J. Niles-Weed, D. Evans, P. Roberts and H.S. Groucutt 2023. Bayesian regression versus machine learning for rapid age estimation of archaeological features identified with lidar at Angkor. *Scientific reports* 131: 17913.

Chevance, J.-B., D. Evans, N. Hofer, S. Sakhoeun and R. Chhean 2019. Mahendraparvata: an early Angkor-period capital defined through airborne laser scanning at Phnom Kulen. *Antiquity* 93: 1303-1321.

Cody, T.R. and S.L. Anderson 2021. LiDAR predictive modeling of Pacific Northwest mound sites: a study of Willamette Valley Kalapuya Mounds, Oregon (USA). *Journal of Archaeological Science, Reports* 38: 103008.

Cohen, A., S. Klassen and D. Evans 2020. Ethics in archaeological lidar. *Journal of Computer Applications in Archaeology* 3: 76-91.

DJI 2023. *DJI L1 Operation Guidebook*, v. 1.2. Shenzhen: DJI Technology Co.

Eisenbeiss, H., M. Sauerbier, L. Zhang and A. Gruen 2005. Mit dem Modellhelikopter über Pinchango Alto. *Geomatik Schweiz* 9: 510-515.

Eisenbeiss, H. and L. Zhang 2006. Comparison of DSMs generated from mini UAV imagery and terrestrial laser scanner in a cultural heritage application. *The International Archives of the Photogrammetry, Remote Sensing and Spatial Information Sciences* 36: 90-96.

Ekaso, D., F. Nex and N. Kerle 2020. Accuracy assessment of real-time kinematics (RTK) measurements on unmanned aerial vehicles (UAV) for direct geo-referencing. *Geo-spatial information science* 23: 165-181.

Evans, D.H. 2016. Airborne laser scanning as a method for exploring long-term socio-ecological dynamics in Cambodia. *Journal of Archaeological Science* 74: 164-175.

Evans, D.H., R.J. Fletcher, C. Pottier, J-P. Chevance, D. Soutif, B.S. Tan, S. Im, D. Ea, T. Tin, S. Kim, C. Cromarty, S. De Greef, K. Hanus, P. Bâty, R. Kuszinger, I. Shimoda and G. Boornazian 2013. Uncovering archaeological landscapes at Angkor using lidar. *PNAS* 110: 12595-12600.

Fontana, G. 2022. Italy's hidden hillforts: a large-scale lidar-based mapping of Samnium. *Journal of Field Archaeology* 47: 245-261.

Fontana, G. 2025. Issues of sampling and representativeness in large-scale LiDAR-derived archaeological surveys in Mediterranean contexts. *Archaeological Prospection* 32: 103-117.

Frachetti, M.D., J. Berner, X. Liu, E.R. Henry, F. Maksudov and T. Ju 2024. Large-scale medieval urbanism traced by UAV–lidar in highland Central Asia. *Nature* 634: 1118-1124.

Garrison, T.G., A.E. Thompson, S. Krause, S. Eshleman, J.C. Fernandez-Diaz, J.D. Baldwin and R. Cambranes 2023. Assessing the lidar revolution in the Maya lowlands: A geographic approach to understanding feature classification accuracy. *Progress in Physical Geography: Earth and Environment* 47: 270-292.

Georgiou, A. 2024. New Silk Road survey reveals hundreds of medieval structures. *Newsweek*, 23 October. Available at: https://www.newsweek.com/archaeologists-reveal-hundreds-medieval-structures-famous-silk-road-1973783

Gustavsson, H-O. 2022. Laserskanning rapport Grenland Vestfold 10 pkt 2022. Unpublished report, Oslo: Terratec.

Guyot, A., M. Lennon, T. Lorho and L. Hubert-Moy 2021. combined detection and segmentation of archeological structures from LiDAR data using a deep learning approach. *Journal of Computer Applications in Archaeology* 4: 1-19.

Hale, J.W.C., D.S. Davis and M.C. Sanger 2023. Evaluating the archaeological efficacy of bathymetric LiDAR across oceanographic contexts: a case study from Apalachee Bay, Florida. *Heritage* 6: 928-945.

Handwerk, B. 2022. Lost Cities of the Amazon Discovered from the Air. *Smithsonian Magazine,* 25 May. Available at: https://www.smithsonianmag.com/science-nature/lost-cities-of-the-amazon-discovered-from-the-air-180980142/.

Hill, A.C. 2019. Economical drone mapping for archaeology: comparisons of efficiency and accuracy. *Journal of Archaeological Science, Reports* 24: 80-91.

Hill, A.C., F. Limp, J. Casana, E.J. Laugier and M. Williamson 2019. A new era in spatial data recording: low-cost GNSS. *Advances in Archaeological Practice* 7: 169-177.

Julge, K., A. Ellmann and A. Gruno 2014. Performance analysis of freeware filtering algorithms for determining ground surface from airborne laser scanning data. *Journal of Applied Remote Sensing* 8(1): 085098.

Kartverket 2017. *Posisjonstjenester i sanntid: referansestasjoner og tjenester*. Oslo: Statens kartverk.

Kersten, T., J. Wolf and M. Lindstaedt 2022. Investigations into the accuracy of the UAV system DJI Matrice 300 RTK with the sensors Zenmuse P1 and L1 in the Hamburg test field, *The International Archives of the Photogrammetry, Remote Sensing and Spatial Information Sciences* 43: 339-346.

Khan, S., L. Aragão and J. Iriarte 2017. A UAV–lidar system to map Amazonian rainforest and its ancient landscape transformations. *International Journal of Remote Sensing* 38: 2313-2330.

Kokalj, Ž. and R. Hesse 2017. *Airborne Laser Scanning Raster Data Visualization: A Guide to Good Practice*. Ljubljana: Založba ZRC.

Kokalj, Ž. and M. Somrak 2019. Why Not a Single Image? *Remote Sensing* 11(747): 1-26.

Letard, M., D. Lague, A. Le Guennec, S. Lefèvre, B. Feldmann, P. Leroy, D. Girardeau-Montaut and T. Corpetti 2024. 3DMASC: accessible, explainable 3D point clouds classification. Application to bi-spectral topo-bathymetric lidar data. *ISPRS Journal of Photogrammetry and Remote Sensing* 207: 175-197.

Levitan, R., E.I. Levine, D. Athanasoulis, I. Legaki, H.R. Indgjerd, E.R. Campbell, J. Vanden Broeck-Parant, J. Paga, V. Anevlavi, T. Jakobitsch and F. Liard *forthcoming*. An Interdisciplinary Workflow for the Comprehensive Study of Ancient Quarried Landscapes. *Antiquity*.

McCoy, M.D., J. Casana, A.C. Hill, E.J. Laugier, M.A. Mulrooney and T.N. Ladefoged 2021. Unpiloted Aerial Vehicle Acquired Lidar for Mapping Monumental Architecture. *Advances in Archaeological Practice* 9: 160-174.

Murtha, T.M., E.N. Broadbent, C. Golden, A. Scherer, W. Schroder, B. Wilkinson and A.A. Zambrano 2019. Drone-mounted lidar survey of Maya settlement and landscape. *Latin American Antiquity* 30: 630-636.

Nesbakken, A. and O. Risbøl 2014. The burial cairns at Mølen – Remote sensing used for change detection in a protected site. *Kart og Plan* 74: 134-149.

Norstedt, G., A.L. Axelsson, H. Laudon and L. Östlund 2020. Detecting cultural remains in boreal forests in Sweden using airborne laser scanning data of different resolutions. *Journal of Field Archaeology* 45: 16-28.

Podobnikar, T. and A. Vrečko 2012. Digital elevation model from the best results of different filtering of a LiDAR point cloud. *Transactions in GIS* 16: 603-617.

Prümers, H., C.J. Betancourt, J. Iriarte, M. Robinson and M. Schaich 2022. Lidar reveals pre-hispanic low-density urbanism in the Bolivian Amazon. *Nature* 606(7913): 325-328.

Rannard, G. 2024. Lost Mayan city found in Mexico jungle by accident. *BBC News*. 29 Oct. Available at: https://www.bbc.co.uk/news/articles/crmznzkly3go

Risbøl, O. and L. Gustavsen 2016. *Bruk av luftbåren laserskanning (lidar) i arkeologien*. Oslo: Riksantikvaren.

Risbøl, O. and L. Gustavsen 2018. LiDAR from drones employed for mapping archaeology: potential,

benefits and challenges. *Archaeological Prospection* 25: 329-338.

Sapirstein, P. and S. Murray 2017. Establishing best practices for photogrammetric recording during archaeological fieldwork. *Journal of Field Archaeology* 42: 337-350.

Schuetz, M. 2016. Potree: Rendering large point clouds in web browsers. Unpublished dissertation, Vienna University of Technology.

Solli, P. 2008. Rapport laserskanning gravhauger Mølen i Larvik. Unpublished report, Oslo: Terratec.

Štular, B. and E. Lozić 2020. Comparison of filters for archaeology-specific ground extraction from airborne LiDAR point clouds. *Remote Sensing*. 12(18): 3025.

Štular, B., E. Lozić and S. Eichert 2021. Airborne LiDAR-derived digital elevation model for archaeology. *Remote Sensing* 13(9): 1855.

Tapete, D., A. Traviglia, E. Delpozzo and F. Cigna 2021. Regional-scale systematic mapping of archaeological mounds and detection of looting using COSMO-SkyMed high resolution DEM and satellite imagery. *Remote Sensing* 13(16): 3106.

Torsnes, A. 2017. Laserskanning for nasjonal detaljert høydemodell NDH Larvik 5 pkt 2017. Unpublished report, Oslo: Terratec.

Verschoof-van der Vaart, W.B., K. Lambers, W. Kowalczyk and Q.P. Bourgeois 2020. Combining deep learning and location-based ranking for large-scale archaeological prospection of LiDAR data from the Netherlands. *ISPRS International Journal of Geo-Information* 9(5): 293.

Vinci, G., F. Vanzani, A. Fontana and S. Campana, S. 2024. Lidar applications in archaeology: a systematic review. *Archaeological Prospection* 32: 82-101.

Zakšek, K., K. Oštir and Ž. Kokalj 2011. Sky-view factor as a relief visualization technique. *Remote Sensing* 3: 398-415.